

---

# Study of adhesive joints under static and fatigue loading

**Baramée Patamaprohm<sup>1</sup>, Ekkarin Phongphinitana<sup>2</sup>,  
Clément Guinault<sup>1</sup>, Vladimir Gantchenko<sup>1</sup>, Jacques Renard<sup>1</sup>,  
Jean-Pierre Jeandrau<sup>3</sup>, Catherine Peyrac<sup>4</sup>, Fabien Lefebvre<sup>4</sup>**

1. Centre des Matériaux P.M. Fourt  
Mines-Paris Tech, CNRS UMR 7633  
BP87, F-91003 Evry cedex, France
2. Department of Mechanical and Aerospace Engineering  
DMIE Center, King Mongkut's University of Technology North Bangkok  
1518 Pibulsongkram Rd., Bangsue, Bangkok 10800, Thailand
3. CETIM Saint-Étienne, 7 Rue de la Presse, 42000 Saint-Étienne, France
4. CETIM Senlis, 52 Avenue Félix Louat, 60300 Senlis, France

*baramee.patamaprohm@mines-paristech.fr*

---

*ABSTRACT. This study deals with the characterization of two adhesive joints under quasi static and fatigue loading. Different testing systems were involved. For quasi static loading, the complex behaviour model based on modified Drucker-Prager criterion taken into account hydrostatic stress and rate dependence was proposed to describe the elasto-visco-plastic behaviour of adhesives. The model's parameters were determined and validated from experiments with the aid of finite element simulations (FEM). For fatigue loading, the lifetime of adhesives was studied. S-N curves was established and extended a failure criterion for any number of cycles. Endurance limit was determined for any combination of applied load for one adhesive, while another adhesive showed the endurance limit only in shear loading.*

*RÉSUMÉ. Le collage structural, technologie d'assemblage par adhésion, est apparu il y a moins d'un siècle. Présent dans tous les domaines de l'industrie et en particulier dans celui des transports, son développement est principalement dû à un avantage considérable : son utilisation permet de réaliser des gains de masse. En effet il permet d'assembler des matériaux difficilement assemblables : par exemple les composites et les métalliques. Dans ce but, de nombreuses études ont été menées afin d'identifier le comportement du collage structural et d'en assurer les performances, en visant une application bien précise. À l'heure actuelle certaines performances ne sont pas totalement maîtrisées, dont la prédiction du comportement sur le long terme. Ce point, en phase de conception, est essentiel pour l'industrie. De plus, l'absence de normes concernant la caractérisation des assemblages collés constitue une barrière pour la maîtrise de cette technologie. C'est autour de cette problématique que notre étude a été réalisée. Dans ce travail, nous avons caractérisé deux adhésifs en sollicitation quasi statique et en sollicitation de fatigue. Différents types d'essais*

*ont été effectués, (essais de traction, essais Arcan-Mines, essais TAST et essais de simple recouvrement). Pour le comportement quasi statique, un critère de Drucker-Prager modifié, prenant en compte la sensibilité à la contrainte hydrostatique et à la vitesse de sollicitation, est proposé pour décrire le comportement d'adhésifs du type visco-élasto-plastique, lors de sollicitations complexes. Les paramètres du modèle ont été identifiés lors des essais mécaniques et validés à l'aide de simulations par élément finis. La durée de vie du collage en fatigue répétée a été étudiée avec plusieurs types de sollicitations : cisaillement pur, cisaillement et contraintes normales, traction triaxiale. Les courbes de Wöhler obtenues nous ont permis d'établir un critère généralisé, de rupture en fatigue, pour différents nombres de cycles donnés. La limite d'endurance a été déterminée pour l'un des adhésifs pour toute combinaison des charges appliquées, alors que l'autre adhésif montrait une limite d'endurance uniquement pour la sollicitation en cisaillement.*

*KEYWORDS: Drucker-Prager criterion, adhesive joint assembly, FEM simulations, fatigue.*

*MOTS-CLÉS : critères de Drucker-Prager, collage structural, simulations par éléments finis, fatigue multiaxiale.*

DOI:10.3166/RCMA.26.63-85 © 2016 Lavoisier

## 1. Introduction

Adhesive joint is a structural assembly technology which has been widely used in many industrial sectors and particularly transportation. Comparing to others assembly technologies such as riveted mechanical locking (which is not recommended for composites), the adhesive joint takes an advantage in weight reduction which is the motivation of reducing energy consumption in transportation. In addition for the objective of weight reduction, the application of lightweight materials such as polymer-matrix composites (2.7 or 7.8 times lighter than aluminium or steel respectively) for structural parts and partially substituting steel is expected. As a result, most engineering structures will be made of multi-components including several types of materials. Then the main important question for the adhesive joint technology is how to join dissimilar materials or structural parts, how to characterize assembly zones and model them. The stability of the joint, its life-time and its durability become an essential knowledge for industrial conception design. However, knowledge in some area is still lacking until now, long term behaviour prediction in particular.

In the context of this study, we aim to propose a methodology for characterize and modelling an adhesive joint subjected to static and fatigue loading. For adhesive studies, a “cohesive” failure is required for guarantee the identified properties coming from an adhesive itself. A cohesive failure refers to the failure within the joint while an adhesive failure stand for the interface failure between adhesive joint and it substrate which depends on a substrate material. The choice of adhesive from industrial provides this preferable cohesive failure and leads to a particular criterion. The two studied polymer base adhesives in this study show a complex elasto-viscoplastic behaviour. The model based on modified Drucker-Prager criterion has been proposed and taken into account the hydrostatic stress and rate dependence. In static

loading, four different tests (tensile test, Arcan-Mines test, TAST and single laps shear test) were involved in order to characterize and validate the model's parameters along with the FEM simulations. For fatigue loading, we aim to study the life time of adhesive joint. This fatigue work purely dedicated to experiments, no FEM simulation was involved. Arcan-Mines tests were mainly performed in order to extend the modified Drucker-Prager failure criterion for any number of cycles. Fatigue tests were also monitored on TAST and single lap shear specimens as a comparison to the shear mode Arcan-Mines test ( $90^\circ$ ). S-N curves (Wöhler curves) and fatigue endurance limits (maximum loads for running 107 cycles without failure of adhesive joint) were finally obtained.

## 2. Materials

In this study, two adhesives were investigated. (i) Sika Power 4588, fabricated by Sika Power for automotive industrial applications, is a thixotropic mono component adhesive with hybrid epoxy/polyurethane base for the purpose of high resistance and good adherence with a greasy surface. This adhesive cures at high temperature,  $180^\circ\text{C}$  during 30 minutes. (ii) Aderis 8641-1107, fabricated by Jacret, is a bi-component adhesive with methacrylate base. This adhesive is reasonably stable for a wide temperature range which is favourable to automotive industrial. Although, this adhesive is capable to polymerise at room temperature, the polymerization process in this study was recommended by our industrial partner to cure at  $170^\circ\text{C}$  during 60 minutes. As mechanical properties of these two adhesives dominate by their viscosity, the elasto-visco-plastic behaviour model was chosen. Time and pressure dependence to plastic strain were also taken into account.

## 3. Overview of experiments

Several testing systems were conducted in this study and most of them were performed both on static and fatigue loading: (i) tensile tests, (ii) Arcan-Mines tests with different loading conditions, (iii) Thick Adherent Shear Tests (TAST) and (iv) single lap shear tests. While, tensile tests use a typical bulk specimen (dog bone shape), the last three tests use their own specific specimens designated for adhesive joint testing (Figure 1). For Arcan-Mines specimens, beaks at the edge of specimen reduce efficiently the stress concentration and peeling stress close to free surfaces. The setups of each test demonstrate in Figure 2. The strains of bulk adhesive were followed both in longitudinal and transversal directions in case of tensile tests (Figure 2a). Arcan-Mines test is a specific setup inspired by the previous work of Arcan (Arcan *et al.*, 1978). The modified version by Mines allows the fixture to vary the angle as a result in different applied loading condition (Bassery *et al.*, 2010 ; Joannès *et al.*, 2010 ; Bassery et Renard, 2012). While direction  $0^\circ$  and  $90^\circ$  represent the tri-axial and pure shear state of stress respectively, directions  $30^\circ$  and  $60^\circ$  stand for the combination of tensile-shear state of stress (Figure 2b). Different loading conditions characterize the hydrostatic stress dependency of material, each direction induces the different pressure field on the joint. The deformations were measured by

specific extensometers located on the metallic substrates close to the joint. TAST is a test which relatively similar to Arcan-Mines test at 90° (Cognard *et al.*, 2008), its specimen is an evolution of single lap shear specimen. The thickness of substrates is more significant than the single lap shear in order to prevent their bending. Extensometers are located on both sides of specimens (Figure 2c). Single lap shear test is the most widespread shear test in industrial. This test is relative sample to implement, both in term of preparation and realization of the test. However, the thickness and offset of substrates induce their bending and create a heterogeneous and complex stress field within the joint (Figure 2d).

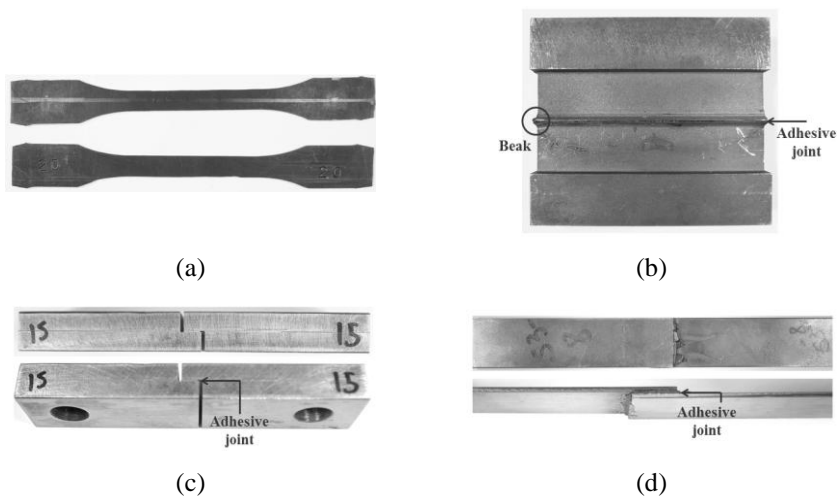


Figure 1. Different testing specimens: (a) tensile test, (b) Arcan-Mines test, (c) TAST and (d) Single lap shear test

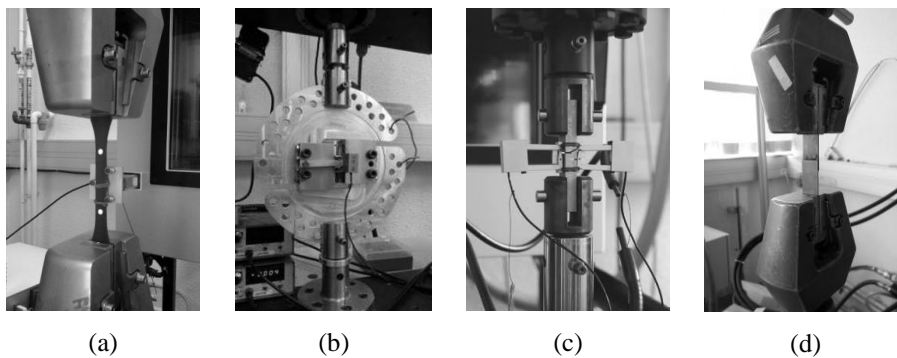


Figure 2. Different testing setups: (a) tensile test, (b) Arcan-Mines test, (c) TAST and (d) Single lap shear test

#### 4. Static case

For static case, the main objective is to characterize the material properties and propose behaviour model. All four tests get involved. Tensile and Arcan-Mines tests are for parameter's identification while TAST and single lap shear are used to validate the model.

##### 4.1. Model selection

In general for polymers, behaviour model consists of linear elastic domain and non-linear plastic domain due to the influence of viscosity. It can be interpreted by a type of elasto-visco-plastic behaviour. Concerning to elastic domain, we suppose an isotropic behaviour, 2 parameters need to be identified: Young's modulus (E) and Poisson's ratio ( $\nu$ ). The shear modulus can be simply obtained by an isotropic relation. For non-linear plastic domain, the viscoplastic behaviour depends on hydrostatic stress and plastic strain rate. Five principal elements are required to derive a model: (i) plastic criterion, (ii) flow rule, (iii) hardening rule, (iv) rate dependence rule and (v) failure criterion.

##### Plastic criterion

The modified Drucker-Prager yield criterion (Eq(1)) (Drucker et Parger, 1952) has been chosen in this study. The yield surface in the form of parabola in  $I_1$ - $J_2$  plane, (Figure 3) shows the dependence on hydrostatic stress ( $I_1$ ) (Caddell *et al.*, 1974). The criterion's parameters are identified by Arcan-Mines tests in different directions ( $0^\circ$ ,  $30^\circ$ ,  $60^\circ$  and  $90^\circ$ ). The experimental data are treated by equations (2-4) where F is a force at yield limit and S is a specimen cross section in which it yield point justified by loss of linearity in experimental curve.

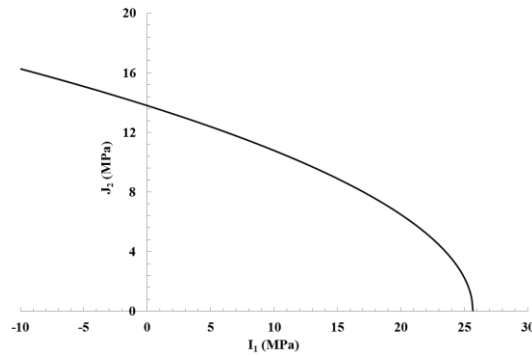


Figure 3. Yield surface: modified Drucker-Prager

$$f = (J_2)^2 - A + BI_1 = 0 \quad (1)$$

$$I_1 = \sigma_{11} + \sigma_{22} + \sigma_{33} \quad (2)$$

$$J_2 = \sqrt{((\sigma_{11} - \sigma_{22})^2 + (\sigma_{22} - \sigma_{33})^2 + (\sigma_{33} - \sigma_{11})^2 + 6(\sigma_{12}^2 + \sigma_{13}^2 + \sigma_{23}^2))/2} \quad (3)$$

$$\sigma_{11} = \frac{F}{S} \cos(\theta), \sigma_{22} = \sigma_{33} = \frac{\nu}{1-\nu} \frac{F}{S} \cos(\theta), \sigma_{12} = \frac{F}{S} \sin(\theta) \text{ and } \sigma_{13} = \sigma_{23} = 0 \quad (4)$$

*Flow rule*

In plasticity, the relation of stress and plastic strain rate is defined by the flow rule (Eq.5). With F, the potential flow equal to the yield surface function, we have an associated plastic flow which is a better choice. However, due to the limit of FEM software, the use of this yield surface function is unavailable. The potential flow needs to be defined otherwise and different form the yield surface leading to a non-associated plastic flow. In FEM software Abaqus, a hyperbolic function (Eq.6) is available.  $\xi$  is a eccentricity defined an approaching rate of function to its asymptotes. This parameter is identified with respect to  $dF \cong df$ . Next,  $\Psi$  stands for a friction angle of material. This angle can be measured at high confining hydrostatic pressure state in  $(-I_1/3)$ - $J_2$  plane (Figure 4) in which  $-I_1/3$  refers to a hydrostatic pressure (p).

$$d\epsilon_{ij}^p = d\lambda \frac{\partial F}{\partial \sigma_{ij}} \quad (5)$$

$$F = \sqrt{(\xi \sigma_y \tan \psi)^2 + (J_2)^2} + \frac{I_1}{3} \tan \psi \quad (6)$$

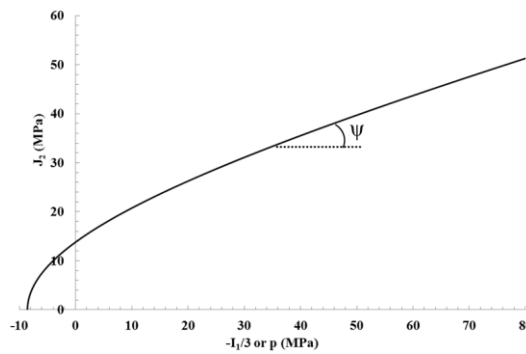


Figure 4. Friction angle in  $(-I_1/3)$ - $J_2$  plane

In order to identify the friction angle, we made the hypothesis that this angle is equal to the dilatation angle of material ( $\beta$ ), (Charalambides et Olusangya, 1997).

The dilatation angle refers to the ratio of volumetric plastic strain to Von Mises equivalent plastic strain and can be determined by Eq.7 where plastic Poisson's ratio ( $v^p$ ) obtained from tensile test. This angle refers to an increasing in volume during plastic flow. In case of metallic material, volume is constant during plastic flow, the plastic Poisson's ratio go to 0.5 and results in  $\beta=0$ .

$$\tan\psi \cong \tan\beta = \frac{I'_1}{J'_2} = \frac{\varepsilon_{11}^p + \varepsilon_{22}^p + \varepsilon_{33}^p}{\sqrt{\frac{2}{3} \varepsilon_{ij}^p : \varepsilon_{ij}^p}} = \frac{3(1-2v^p)}{2(1+v^p)}, \text{ (cases of tensile test)} \quad (7)$$

#### *Hardening rule*

If the material is harden-able, the yield surface will change its form or position during plastic flow with respect to plastic strain. We have been selected the non-linear isotropic hardening for our model. In case of monotonic loading, the mechanical response can be described by Eq.8. This rule is implemented in software Abaqus by multi-linear manner. The parameters are identified by Arcan-Mines test at  $90^\circ$  represented pure shear loading condition.

$$\sigma_{eq} = \sigma_y + H\varepsilon_{eq}^p + Q(1 - e^{-b\varepsilon_{eq}^p}) \quad (8)$$

#### *Rate dependence rule*

For our adhesives, a viscosity effect related to a dependence of the properties to strain rate and cannot be neglected. We have been chosen the model that separates effect of strain rate and strain. The model supposes that a hardening depended on strain rate can be defined by the single "static" hardening curve and a scaling scalar factor. It is a power law that available in software Abaqus (Eq.9). The parameter D and n are identify from the Arcan-Mines tests at  $90^\circ$  with different crosshead speed with a hypothesis that behaviour at strain rate of 0.0001s<sup>-1</sup> being a static case.

$$\sigma_{eq} = \sigma_{eq} \Big|_{\dot{\varepsilon}_{eq}^p=0} \left( 1 + \left( \frac{\dot{\varepsilon}_{eq}^p}{D} \right)^{\frac{1}{n}} \right) \quad (9)$$

#### *Failure criterion*

A modified Drucker Prager criterion has been assigned to describe the failure of adhesives. The second parabola defines a failure region for given adhesive joint. Depending on the plastic strain rate, the viscosity modifies this parabola. Two parameters of the criterion need to be expressed in function of plastic strain rate. According to the experimental results, the failure stress from Arcan-Mines test at  $90^\circ$  depended on loading rate while Arcan-Mines test at  $0^\circ$  showed the failure stress less depended on loading rate. By consequence, we assume  $I_1$  at  $J_2=0$  is constant and independent to plastic strain rate. The evolution of failure parabola demonstrates in Figure 5a. The second point is a state of hydrostatic pressure (represented by  $I_1$ ) on

Arcan-Mines test at 90°. This test represents the pure shear state of stress in which  $I_1$  is null. However if we use a viscoplastic model that sensitive to hydrostatic pressure, material volume will increase theoretically during the plastic flow for any loading (Besson *et al.*, 2001). During the test, an adhesive joint is confined and its volume is considerably constant. Therefore, the addition compression needs to be taken into account in order to maintain the volume constant.  $I_1$  is no longer null but go to negative (Figure 5b). We identify this additional compression by the simulation aiding.

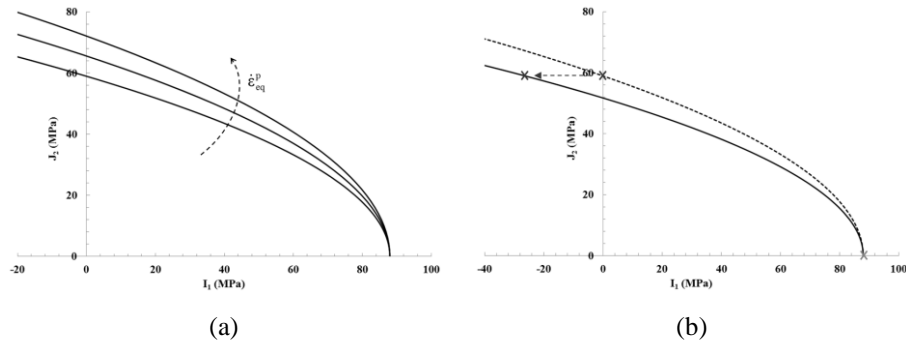


Figure 5. (a) Evolution of failure surface with respect to plastic strain rate, (b) Modification of failure surface by taking into account a dilatation of volume

#### 4.2. Identification of model's parameters

##### Tensile tests

Tensile tests were carried out in order to identify Young's modulus ( $E$ ), Poisson's ratio ( $\nu$ ) and plastic Poisson's ratio ( $\nu^p$ ). Young's modulus is the linear slope at the beginning of the experimental curve (Figure 6a). Poisson's ratio is the average of negative ratio of transverse to axial strain. For the plastic Poisson's ratio, an elastic part needs to be removed. With the Eq. (10-12), we obtain the true stress in function of true plastic strain curve (Figure 6b) using for determine an average plastic Poisson's ratio. The identified properties are summarised in Table 1.

$$\epsilon^p = \epsilon - \epsilon^e = \epsilon - E\sigma \quad (10)$$

$$\sigma_{\text{true}} = F/S = Fl/(S_0l_0) = F(\Delta l + l_0)/(S_0l_0) = F/S_0(1 + \Delta l/l_0) = \sigma(1 + \epsilon) \quad (11)$$

$$\epsilon_{\text{true}} = \int_{l_0}^l \delta l/l = \ln(l/l_0) = \ln((\Delta l + l_0)/l_0) = \ln(1 + \Delta l/l_0) = \ln(1 + \epsilon) \quad (12)$$

Table 1. Summary of identified parameters

	E (MPa)	$\nu$	$\nu^p$
Sika Power	2272	0.4	0.36

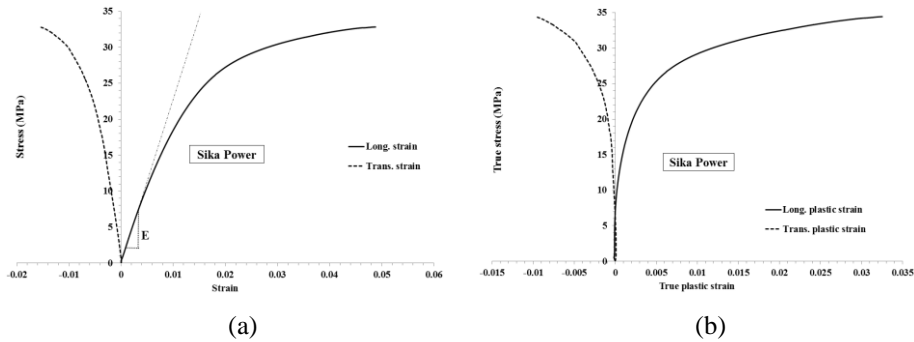


Figure 6. Tensile test curve: (a) stress-strain and (b) true stress-true plastic strain

Others parameters of plastic behaviour were identified from Arcan-Mines tests with the fact that adhesives joint specimens are more representative than bulk specimens. Since the bulk specimens fabricated from Aderis adhesive showed a critical number of porosity, the tensile test for Aderis was abandoned. Its Young’s modulus and Poisson’s ratio was determined by Arcan-Mines tests with the aide of numerical simulations. Only plastic Poisson’s ratio was adopted from Sika Power. This ratio is basically close for the same type of material (polymer).

*Arcan-Mines tests*

Arcan-Mines tests in different directions are essential for the characterization of adhesive joint. The limit elastic was justified by loss of linearity of each experimental curve. Table 2 summarises the identified parameters and the average parabola for elastic limit was established (Figure 7).

Table 2. Summary of identified parameters for the 2 adhesives

$f = (J_2)^2 - A + BI_1$	Elastic limit	
	A (MPa <sup>2</sup> )	B (MPa)
Sika Power	190	7.4
Aderis	115	3.8

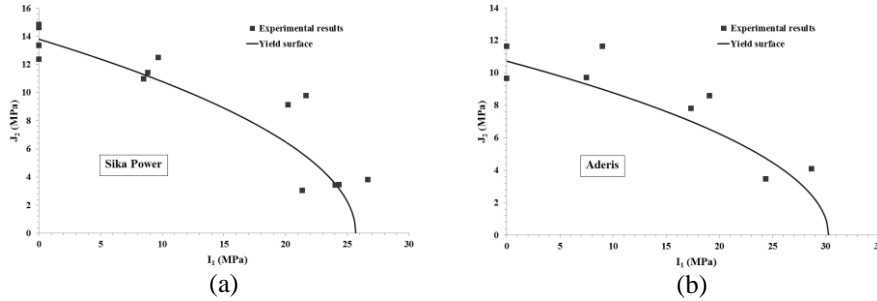


Figure 7. Modified Drucker-Prager yield surface: (a) Sika Power, (b) Aderis

For characterization of plastic behaviour, the 3D FEM simulation of entire setup fixture was conducted taking into account a non-negligible deformation of the fixture and a deformation of metallic substrates. A recording deformation by extensometers was not only from adhesive joint, but also from the metallic substrates. The preliminary parameters of model were analytically calculated then optimized by the simulations. The deformation was exported from the simulations at the same measuring points and compared to the experimental results.

For Arcan-Mines test at  $90^\circ$  referring to the pure shear state, the slope at the beginning of experimental curve cannot represent correctly the shear modulus of adhesive. The presence of beaks on Arcan-Mines specimens conducts a non-uniform stress field (Cognard *et al.*, 2005). However, this stress field trends to become more uniform with the intervening of plasticity (Figure 8). Therefore, we assumed that the experimental curve could represent the adhesive joint after entering to the non-linear plastic region. We note that the beaks have the advantage to eliminate the peeling stress around the edge of specimens a result in improved failure strength (Cognard *et al.*, 2004).

From an experimental curve at  $90^\circ$ , we obtained a domain of plasticity expressed in equivalent stress and equivalent plastic strain using Eq. (14). Concerning to the true stress-strain, the difference between “true” and “engineering” is obvious when there is a significant cross section’s reducing (which is a case of dog-bone specimens in tensile test). On the other hand, the specimen of Arcan-Mines test can be considered to maintain a constant cross section up to failure leading to indifferent in true and engineering stress-strain. Using Eq. (8), we obtained the preliminary parameter for the simulation. After performing several iterations, we finally determined the definitive parameters (Table 3) with have a good agreement with the experimental results (Figure 9). For Aderis, the softening at the end still required more sophisticated hardening model to describe it correctly.

$$\sigma_{eq} = \sqrt{3}\sigma_{12} \quad \text{and} \quad \varepsilon_{eq}^p = \gamma_{12}^p / \sqrt{3} \quad (14)$$

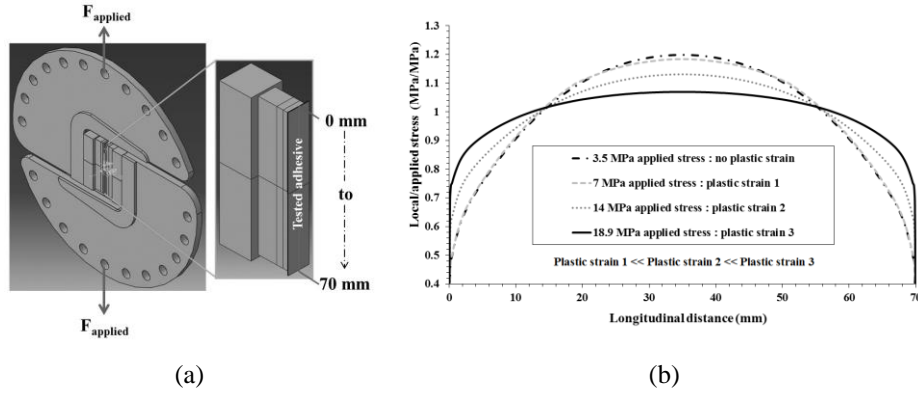


Figure 8. Evolution of stress field in function of plastic strain: (a) observed section and (b) profile of stress field

Table 3. Summary of identified parameters of behaviour model for the 2 adhesives

	E	$\nu$	$\Psi$	$\sigma_y$	b	H	Q	$\xi$	n	D
Sika Power	2272	0.4	16.9	13.8	110	12.6	31.5	8.4	4.7	22.9
Aderis	1250	0.4	16.9	10.7	40	0.8	2.7	5.3	4.9	0.018

In grey: value adopt from Sika Power; E,  $\sigma_y$ , H, Q are in MPa

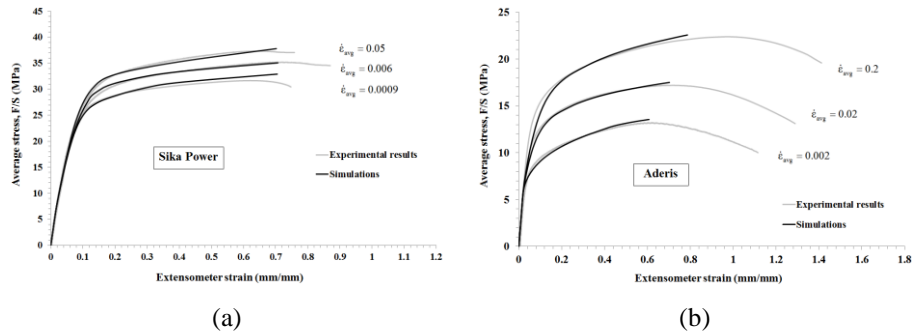


Figure 9. Simulation of Arcan-Mines test at 90°: (a) Sika Power and (b) Aderis

Concerning to a failure of adhesives, two parameters of modified Drucker-Prager for failure criterion were expressed in function of equivalent plastic strain rate ( $\dot{\epsilon}_{eq}^p$ ). This strain rate improved during the test even with constant cross head speed (in

mm/min). By consequence, instead of average strain rate ( $\dot{\epsilon}_{avg}$ ), we used the equivalent plastic strain at ultimate stress. The parabolas for failure of adhesive were finally established (Figure 10). The two parameters of model in function of  $\log(\dot{\epsilon}_{eq}^p)$  demonstrate in Figure 11. The summary of associated parameters shows in Table 4.

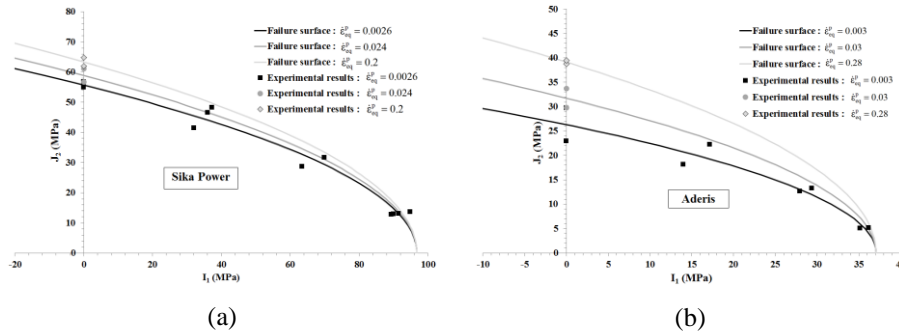


Figure 10. Failure criterion of modified Drucker-Prager: (a) Sika Power and (b) Aderis

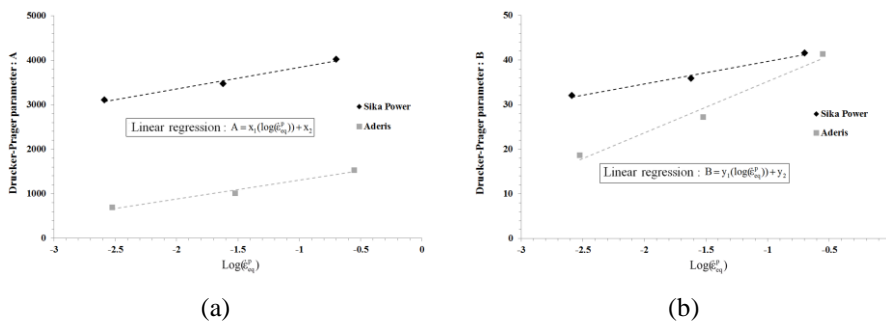


Figure 11. Parameters of failure criterion in function of equivalent plastic strain rate at ultimate stress: (a) A and (b) B

We note that the summarised parameters in Table 4 did not take in to account an additional compression due to an increasing of volume during plastic flow. Although, these parameters can still be used in purely elastic cases focusing simply on the failure of adhesive such as a complicated structural simulation of industrials in which the completed behaviour model of adhesive is not a priory and the elastic simulation is always preferable. With given equivalent plastic strain rate, the parameters in Table 4 are capable to establish the specific failure parabola for elastic simulation.

Table 4. Summary of failure criterion's parameters,  
**WITHOUT additional compression**

$f = (J_2)^2 - A + BI_1$	Cross head speed (mm/min)	$\dot{\epsilon}_{avg} (s^{-1})$	$\dot{\epsilon}_{eq}^p (s^{-1})$	A (MPa <sup>2</sup> )	B (MPa)
Sika Power	0.1	0.0009	0.0026	3102	32.05
	1	0.006	0.024	3469	35.85
	10	0.05	0.2	4019	41.53
Aderis	0.1	0.002	0.003	691	18.66
	1	0.02	0.03	1008	27.20
	10	0.2	0.28	1531	41.31

$f = (J_2)^2 - A + BI_1$	$A = x_1(\log(\dot{\epsilon}_{eq}^p)) + x_2$		$B = y_1(\log(\dot{\epsilon}_{eq}^p)) + y_2$	
	$x_1$	$x_2$	$y_1$	$y_2$
Sika Power	486	4324	5.02	44.68
Aderis	426	1729	11.49	46.66

As mentioned previously for the behaviour model depending on hydrostatic pressure, an increasing of volume is expected and a supplementary compression to keep a volume constant need to be add. However, an analytical formula for this compression is complicated to derive. The numerical simulation was took place for instead. During the simulation, we increased loading to an experimental failure load so that we could determine the average hydrostatic stress (negative  $I_1$  represent the compression). Figure 12 shows the corrected parabolas for this additional compression. The corrected parameters are summarised in Table 5.

Table 5. Summary of corrected failure criterion's parameters,  
**WITH addition compression**

$f = (J_2)^2 - A + BI_1$	$\dot{\epsilon}_{eq}^p (s^{-1})$	$I_{1,corrected}$ for Arcan-Mines 90°, by simulation (MPa)	A (MPa <sup>2</sup> )	B (MPa)
Sika Power	0.0026	-23.69	2492	25.75
	0.024	-23.59	2789	28.82
	0.2	-24.74	3201	33.08
Aderis	0.003	-16.40	479	12.93
	0.03	-15.44	711	19.20
	0.28	-15.76	1074	28.98

$f = (J_2)^2 - A + BI_1$	$A = x_1(\log(\dot{\epsilon}_{eq}^p)) + x_2$		$B = y_1(\log(\dot{\epsilon}_{eq}^p)) + y_2$	
	$x_1$	$x_2$	$y_1$	$y_2$
Sika Power	376	3441	3.88	35.56
Aderis	302	1217	8.14	32.85

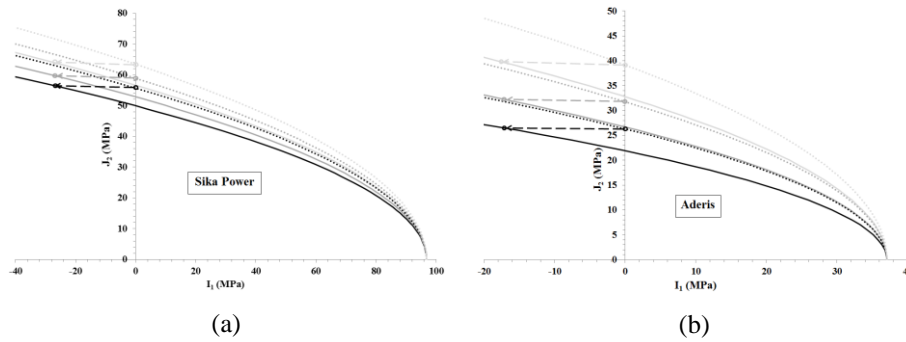


Figure 12. Corrected failure criterion: (a) Sika Power and (b) Aderis

### 4.3. Validation of model

#### TAST and Single lap shear test

TAST and single lap shear test were carried out for the objective of model’s validation. For single lap shear test, we observed that the metallic substrates were permanently bended after loading (Figure 13) which is a sign of the plasticity in substrates. This plasticity was taken into account in the simulation by the non-linear kinematic hardening rule (Lemaitre et Chaboche, 2004). The response to monotonic loading follows Eq. (15) and the associated parameters are summarised in Table 6.

$$\sigma_{eq} = \sigma_y + Q(1 - e^{-b\epsilon_{eq}^p}) \quad (15)$$

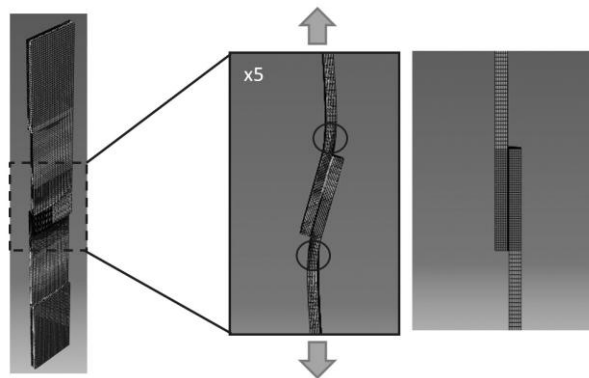


Figure 13. Bending of metallic substrates during single lap shear test

Table 6. Summary of properties of metallic substrates behaviour

E (MPa)	$\nu$	$\sigma_y$ (MPa)	Q (MPa)	b
217830	0.33	200	433	9

The comparison of simulation and experimental results are shown in Figure 14 for TAST and Figure 15 for single lap shear. Overall, the simulation has a good agreement with experimental results. For single lap shear test with Aderis adhesive, the investigation of failure surface shows a lot of porosity for the two weakest results.

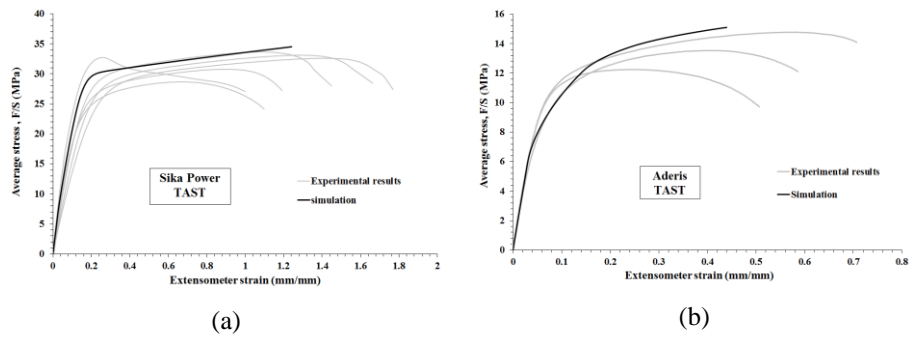


Figure 14. Validation of behaviour model by simulation: TAST

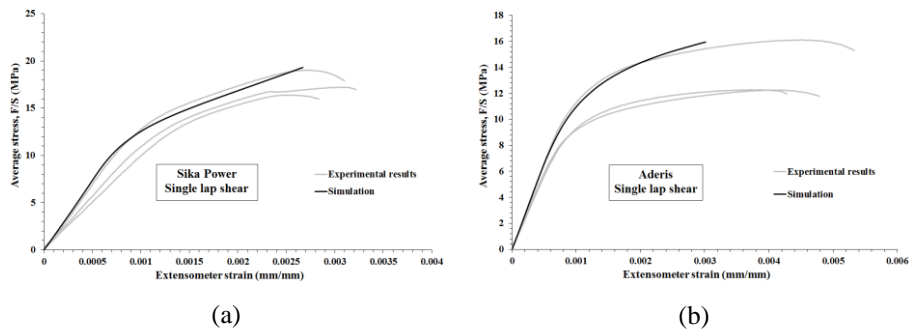


Figure 15. Validation of behaviour model by simulation: single lap shear test

### 5. Fatigue case

For fatigue loading, the objective is to study a lifetime of adhesive joints. Arcan-Mines tests, TAST and single lap tensile shear tests get involved in this study. The

first step is to select the loading frequency. The choice is limited by two constraints, very slow frequency will lead to extremely long time testing, on the other hand very high frequency will cause the self-heating in the adhesive joint and modified its properties. By this reason, the raise of temperature is limited to 5°C higher than room temperature using an infrared camera. The optimized frequency for our fatigue tests is 12 Hz. At this frequency, more than 1 million cycles can be achieved per day which is acceptable in accordance with the overall testing time. During the test, the frequency is progressively increased and will be reached 12 Hz at about 700 cycles. Second step concerns the loading type, a sinusoidal signal coupling with a stress ratio  $R=0.1$  is chosen. The objective is to obtain at least three exploitable points at minimum five levels of stress. The S-N curve, associated to type of loading described previously, is finally established using the ultimate applied stress and the number of failure cycles.

### 5.1. Effect of frequency

In order to verify the frequency effect, the additional Arcan-Mines tests at 90° were carried out at 2 and 5 Hz on Sika Power specimens. The results were similar to the tests at 12 Hz (Figure 16). We concluded that there is no effect of frequency up to 12Hz on the adhesive joint.

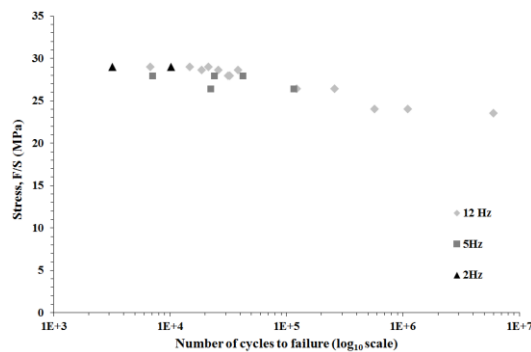


Figure 16. Effect of frequency on Arcan-Mines test at 90° with fatigue loading

### 5.2. S-N curves

#### Arcan-Mines tests

The experimental results from the Arcan-Mines tests in different directions at  $R=0.1$  are demonstrated in Figure 17 for Sika Power and Figure 18 for Aderis including failure and non-failure specimens. For the failure specimens, the failure surface is cohesive. The experimental data denoted “non-failure” refers to the non-failure specimens in which the test was attended to stop for the reason of time saving. They also indicate the proximity of the endurance limit.

A linear regression line was assigned to each group of experimental points with exclude the non-failure points. The endurance limit at  $10^7$  cycles and the standard deviation of points can be estimated from this line. Demonstrating in the Figure 17-18, the two lines correspond to the double of standard deviation shifting from linear regressions.

In case of Sika Power, the endurance limits for different loading configurations were obtained and extended the failure criterion for fatigue loading which demonstrates in the next section. On the other hand, for an adhesive Aderis, only results from Arcan-Mines test at  $90^\circ$  was exploitable for the endurance limit. The repeated test at  $0^\circ$  was conducted, however the scattering of results was still obvious and the S-N curve could not be achieved. Then, we moved on to the Arcan-Mines test at  $30^\circ$ , the same scenario was found. So that, the Arcan-Mines at  $60^\circ$  for Aderis was decided to abandon. Tables 7 and 8 summarized the fatigue results from the Arcan-Mines tests from the two adhesives.

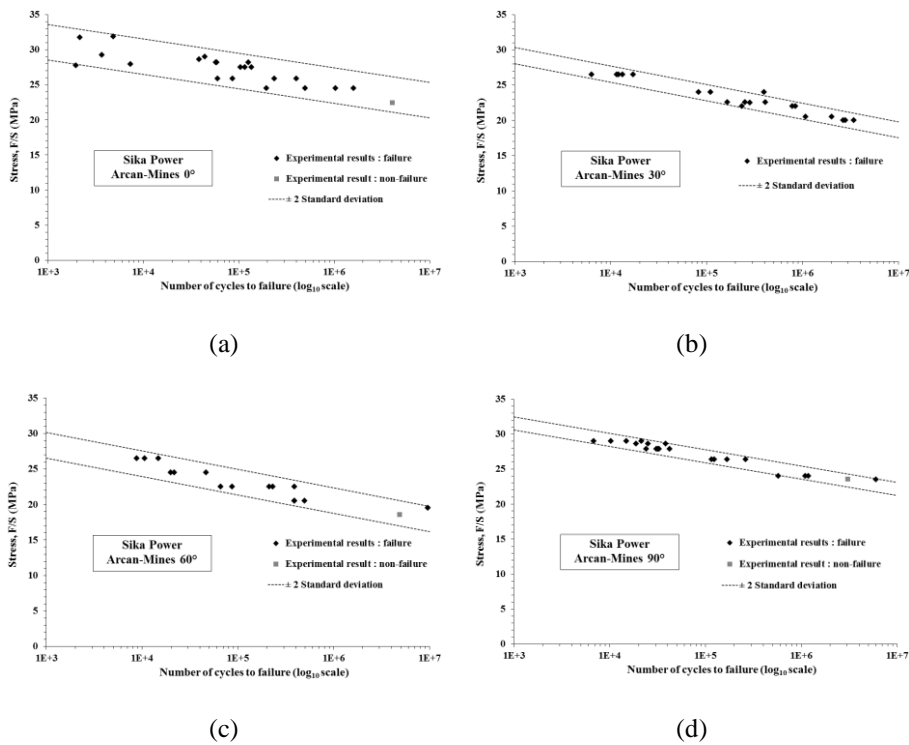


Figure 17. S-N curves for  $R=0.1$  associated to the Arcan-Mines tests: Sika Power

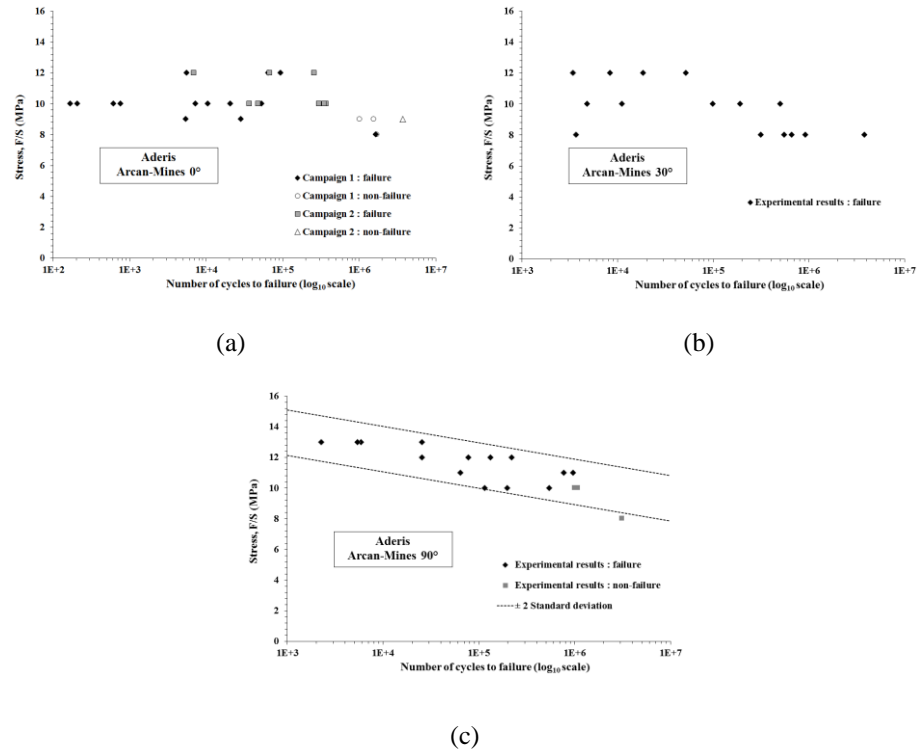


Figure 18. S-N curves for  $R=0.1$  associated to the Arcan-Mines tests: Aderis

Table 7. Summary of fatigue tests: Sika Power

Type of tests	Angle (°)	Number of stress level	Number of tests*	Endurance limit at 7 cycles (MPa)			Standard deviation (MPa)	Coefficient of determination : $R^2$
				$\sigma_D$	$I_1$	$J_2$		
Arcan-Mines	0	5	23 (22)	22.8	51.4	8.5	1.26	0.6484
	30	6	24 (20)	18.7	36.4	17.3	0.57	0.9419
	60	5	19 (16)	17.9	20.2	27.2	0.90	0.8498
	90	6	25 (24)	22.2	0	38.4	0.47	0.9374

(\*) refers to number of tests were used to calculated the linear regression, the failure specimens

Table 8. Summary of fatigue tests: Aderis

Type of tests	Angle (°)	Number of stress level	Number of tests*	Endurance limit at 10 <sup>7</sup> cycles (MPa)			Standard deviation (MPa)	Coefficient of determination : R <sup>2</sup>
				$\sigma_D$	I <sub>1</sub>	J <sub>2</sub>		
Arcan-Mines	0	3	27	N/A			N/A	N/A
	30	3	13	N/A			N/A	N/A
	90	4	18 (17)	9.3	0	16.1	0.74	0.585

(\*) refers to number of tests were used to calculated the linear regression, the failure specimens

5.3. Fatigue failure criterion

Modified Drucker-Prager failure criterion was extended to describe the failure under fatigue loading. The failure criterion was established with analytic equation (Eq.(1-4)) using average failure loads at each direction and cyclic number (Figure 19). We found that all failure surfaces under fatigue loading were superior to limit elastic in static case. The endurance limit (10<sup>7</sup>) was estimated about 57% to 65% for the 4 direction comparing to the static failure. The two parameters of criteria were expressed in function of cyclic number (N) as shown in Figure 20. Since this work was purely experimental approach, the additional compression mentioning in static cases was not taken into account. We noted that this extended failure criterion require the experimental results in 4 directions so that in case of Aderis, the extended failure criterion could not be proposed.

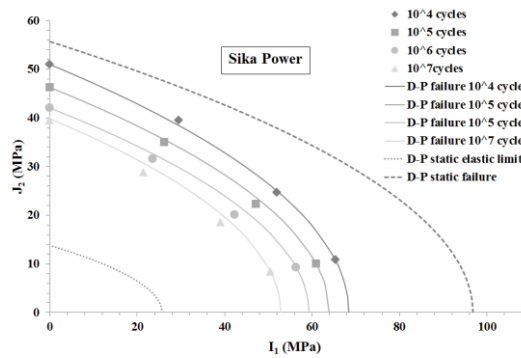


Figure 19. Extension of modified Drucker-Prager criterion for fatigue loading, R=0.1; Sika Power

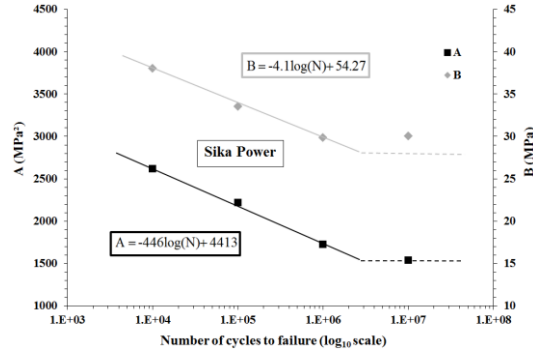


Figure 20. Variation of criterion's parameters in function of cyclic numbers: Sika Power

#### 5.4. Shear tests comparison

As the same objectives as Arcan-Mines test at 90°, TAST and single lap shear test aim to characterize the shear property of adhesive joints. In addition, a previous fatigue study (Jeandrau, 2011) carried out on the adhesive joints has shown that the creep and fatigue limits, using the TAST specimens, were slightly higher than the “reversibility” limit. For this reason, these two tests are interested to compare to the Arcan-Mines test. The results are shown in the following curves (Figures 21 and 22). The shear stress was calculated with Eq. (4), the same as the Arcan-Mines test. The completed comparisons for the three different tests are shown in Figure 23, Tables 9 and 10.

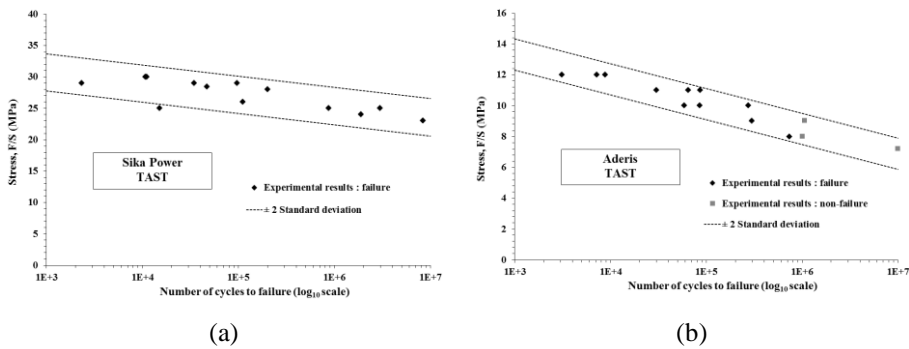


Figure 21. S-N curves for R=0.1 from TAST: (a) Sika Power and (b) Aderis

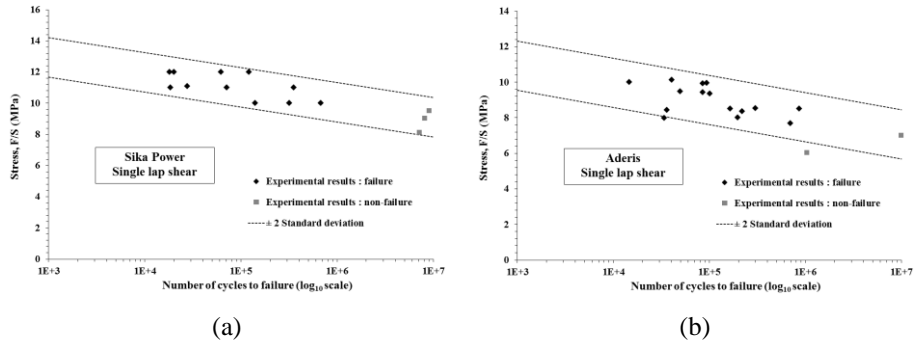


Figure 22. S-N curves for R=0.1 from single lap shear test: (a) Sika Power and (b) Aderis

Table 9. Summary of fatigue shear tests: Sika Power

Type of tests	Angle (°)	Number of stress level	Number of tests*	Endurance limit at 7 cycles (MPa)			Standard deviation (MPa)	Coefficient of determination : R <sup>2</sup>
				$\sigma_D$	I <sub>1</sub>	J <sub>2</sub>		
Arcan-Mines	90	6	25 (24)	22.2	0	38.4	0.47	0.9374
TAST	(90)	6	17 (13)	23.5	0	40.8	1.48	0.6281
Single lap shear	(90)	4	17 (14)	9.1	0	15.8	0.63	0.4168

(\*) refers to number of tests were used to calculated the linear regression, the failure specimens

Table 10. Summary of fatigue shear tests: Aderis

Type of tests	Angle (°)	Number of stress level	Number of tests*	Endurance limit at 7 cycles (MPa)			Standard deviation (MPa)	Coefficient of determination : R <sup>2</sup>
				$\sigma_D$	I <sub>1</sub>	J <sub>2</sub>		
Arcan-Mines	90	4	18 (17)	9.3	0	16.1	0.74	0.585
TAST	(90)	5	20 (17)	6.9	0	11.9	0.51	0.8531
Single lap shear	(90)	4	27 (17)	7.1	0	12.2	0.70	0.3203

(\*) refers to number of tests were used to calculated the linear regression, the failure specimens

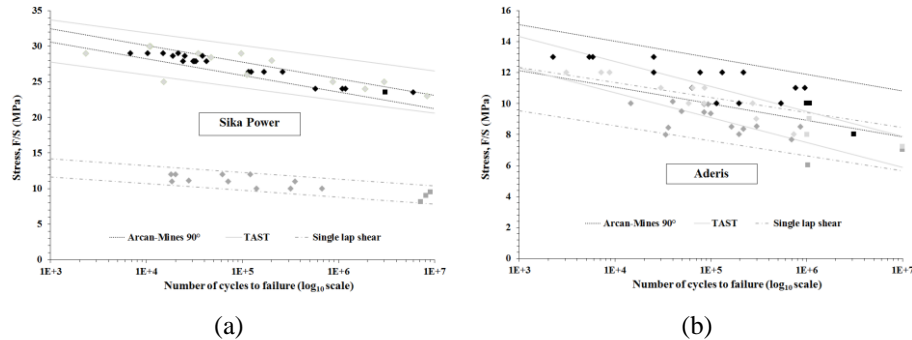


Figure 23. Comparison of different shear tests under fatigue loads,  $R=0.1$ :  
(a) Sika Power and (b) Aderis

For the adhesive Sika Power, the comparison shows that the failure strength on Arcan-Mines and TAST specimens are fairly similar and superior to the static elastic limit while the single lap shears show about three times less. This can be explained by the nature of single lap shear. The heterogeneous stress field including peeling stress induced at the end of jointed zone and rapidly damaged the adhesive joint.

For the adhesive Aderis, the three tests show relative close limit in failure strength. Unlike the Sika Power, the adhesive Aderis has a high level of non-linear behaviour as well as the softening at the end that aid to reduce the heterogeneity of stress field during the plastic flow more obvious than Sika Power. Concerning only on the shear cases, the endurance limit of Aderis can be estimate about 50 to 60% of failure strength in static case.

## 6. Conclusions

This study demonstrates the characterization and modelling of two adhesives under static and fatigue loading. Concerning to static loading, the proposed model based on modified Drucker-Prager criterion is capable to describe the elasto-viscoplastic behaviour of both adhesives. Then, the failure criterion was extended to fatigue loading. Extended Drucker-Prager can describe the failure limit from  $10^4$  cycles up to endurance limit at  $10^7$  in case of Sika Power. The endurance limit was determined for any combination of loading (tension and shear). For Aderis, this adhesive shows the endurance limit only for shear loading. The notably defaults (porosities) observed from the failure Aderis specimens caused the experimental results to be much more scattering than Sika Power. These defaults could prevent the fatigue limit for tension component since tension is more sensitive to porosities than shear component.

### Acknowledgements

We would like to express our gratitude to the CETIM which supported this work through *Etude en fatigue des assemblages collés (Project EFAC)*.

### References

- Arcan M., Hashin Z. et Voloshin A. (1978). A method to produce uniform plane stress states with applications to fiber-reinforced materials. *Experimental Mechanics*, Vol.18 (4), pp. 141-146.
- Bassery J., Ganchenko V. et Renard J. (2010). Caractérisation multiaxiale des interfaces multimatériaux : Application aux assemblages collés. *Revue des composites et des matériaux avancés*, Vol.20 (2), pp. 135-152.
- Bassery J. et Renard J. (2012). Fatigue delamination of carbon fiber fabrics reinforced PPS laminates. *Fatigue Behaviour of Fiber Reinforced Polymers : Experiments and Simulations*.
- Besson J., Cailletaud G., Chaboche J.L. et Forest S. (2001). *Mécanique non linéaire des matériaux*. Hermès-Lavoisier.
- Caddell R.M., Raghava R.S. et Atkins A.G. (1974). Pressure dependent yield criteria for polymers. *Materials Science and Engineering*, Vol.13 (2), pp. 113-120.
- Charalambides M.N. et Olusangya A (1997). *The constitutive models suitable for adhesives in some finite element codes and suggested methods of generating the appropriate materials data*. NPL Report CMMT(B)130, Centre of materials measurement and technology national physical laboratory, UK.
- Cognard J.Y., Davies P. et Sohier L. (2004). Design and Evaluation of bonded composite assemblies. *4<sup>th</sup> European Congress on Computation Methods in Applied Sciences and Engineering*, Jyväskylä, Finland.
- Cognard J.Y., Davies P., Gineste B. et Sohier L. (2005). Development of an improved adhesive test method for composite assembly design. *Composite Science and Technology*, Vol.65, pp. 359-368.
- Cognard J.Y., Créac'hcadec R., Sohier L. et Davies P. (2008). Analysis of the nonlinear behavior of adhesives in bonded assemblies - Comparison of TAST and Arcan tests, *International Journal of Adhesion and Adhesives*, Vol. 28(8), pp. 393-404.
- Drucker D. et Prager W. (1952). Soil mechanics and plastic analysis or limit design. *Quarterly of Applied Mathematics*, Vol.10 (2), pp. 157-165.
- Jeandrau, J-P (2011). Designing adhesively-bonded joints for infinite lifetime when subjected to creep and (or) fatigue loadings. *Fatigue-Design Conference*, Senlis, France.
- Joannès S., Renard J. et Ganchenko V. (2010). The role of talc particles in a structural adhesive submitted to fatigue loadings. *International Journal of Fatigue*, Vol.32 (1), pp. 66-71.
- Lemaitre J. et Chaboche J.L. (2004). *Mécanique des matériaux solides*. 2<sup>e</sup> édition, Dunod.

